Ultrasound-based horizontal ranging in the localization of fetal conus medullaris

Xiuping Liu[a,*], Ping Li[a], Yuemin Yang[a] and Cheng Tian[b]

[a]*Department of Obstetrics and Gynecology, Hebei Medical University Third Hospital, Shijiazhuang, Hebei, China*
[b]*Department of Ultrasound, Hebei Medical University Third Hospital, Shijiazhuang, Hebei, China*

Abstract.

BACKGROUND: Currently, there are a variety of methods for ultrasound to localize the conus medullaris. A concern is that measured values can be influenced by variations in spinal flexion and extension.

OBJECTIVE: To overcome this limitation, the present study measures the horizontal distance (HD) between the end of the conus medullaris and the caudal edge of last vertebral body ossification in normal fetus at different gestational weeks, and analyzes the relationship between the measured value and fetal growth, as well as the utility of these measurements in assessing the position of the conus medullaris.

METHODS: A total of 655 fetuses at gestational weeks 18–40, who underwent routine prenatal ultrasound, were selected in the study. We measured the distance between the end of the cone of the fetal spinal cord and the caudal end of the final vertebral ossification center (Distance1, D1), the distance between the end of the spinal cord cone and the intersection of the extension of D1 with the caudal skin (Distance2, D2), and HD, We analyzed the correlation between the measurements and gestational weeks, established normal reference values, the ratio of D1, D2 and HD to the commonly used growth parameters was calculated. The ratios of D1, D2, HD and the application value of each ratio phase were analyzed, and the reliability analysis of repeated measurement results among physicians was performed.

RESULTS: D1, D2 and HD exhibited strong linear correlations with gestational weeks. Among the ratios of D1, D2 and HD to common growth parameters, D2/FL stabilized after 20 weeks of gestation and consistently exceeded 1. Repeatability tests between D1, D2 and HD showed good reliability ($P > 0.05$).

CONCLUSION: D1, D2 and HD are significantly correlated with gestational age. Horizontal distance measurement can effectively determine the position of fetal conus medullaris, enabling rapid prenatal evaluation of low position of conus medullaris and excluding the possibility of tethered cord.

Keywords: Fetus, ultrasonic examination, conus medullaris, tethered spinal cord

1. Introduction

The conus medullaris is a conical structure located at the distal end of the spinal cord, where the pia mater extends downward as the filum terminale, connecting to the coccyx to provide stability. After the 54th day of embryos, the position of the conus medullaris continuously rises to a relatively high vertebral

*Corresponding author: Xiuping Liu, Department of Obstetrics and Gynecology, Hebei Medical University Third Hospital, No. 139 Ziqiang Road, Qiaoxi District, Shijiazhuang, Hebei 050051, China. E-mail: liuxiuping2023@163.com.

level due to the growth difference between the spinal cord and the spinal column. Finally, the conus medullaris reaches the adult level at birth or within 2 months after birth. The conus medullaris comprises the lumbar sympathetic, sacral nerve and sacral parasympathetic nerves, which extend downwards in the cauda equina [1,2]. Both congenital dysplasia or acquired injuries can cause damage to these nerves, leading to a series of symptoms called tethered cord syndrome (TCS), including abnormalities in the nervous, urinary, musculoskeletal and gastrointestinal systems [3].

For congenital anomalies, early diagnosis and timely treatment are beneficial for the prognosis. The low position of the conus medullaris is closely related to the tethered cord. Advancements in ultrasound technology and the improvement in machine resolution have enabled the visualization of the vertebral canal and internal spinal cord echoes [4]. According to the International Society of Ultrasound in Obstetrics and Gynecology (ISUOG) Practice Guidelines (updated), during the second and third trimesters of pregnancy, the conus medullaris is usually located at the level of the second/third lumbar vertebra (L2-L3) in ultrasound examination of the fetal central nervous system [5]. Due to its cost-effectiveness, repeatability, and ease of use, ultrasound has become the preferred method for assessing the position of the fetal conus medullaris. Prenatal ultrasound evaluations provide valuable information to determine the likelihood of TCS in fetuses. Currently, there are a variety of methods for ultrasound to localize the conus medullaris, including vertebral body localization, renal pole localization, ranging and three-dimensional ultrasound-based localization [6]. Each method has its own advantages and limitations. In practical operations, two-dimensional ranging is widely applied because of its simplicity and rapidity.

A previous study [7] has demonstrated that the length of the root canal increases by 7% when the spine is in a flexed position. As a result, the measured values can be influenced by variations in spinal flexion and extension [8]. To overcome this limitation, the present study proposes a horizontal ranging method for localizing the conus medullaris. Horizontal ranging is not influenced by the physiological curvature of the spine, characterized by more accurate measurement and simple operation. The study quantitatively evaluates the position of the conus medullaris by measuring the horizontal distance (HD) between its end and the caudal end of the ossification center of the terminal vertebral body. In addition, the value of ranging in evaluating the position of the conus medullaris was further analyzed by quantitatively measuring the position of the conus medullaris.

2. Materials and methods

2.1. Subjects

Fetal ultrasound images of pregnant women undergoing routine prenatal ultrasound examinations at Hebei Medical University Third Hospital were collected from March 2020 to February 2021. Initially, 662 cases were collected, of which 7 did not meet the inclusion criteria and were excluded. Finally, 655 cases were enrolled in the study. The gestational age of the fetuses ranged from 18 to 40 weeks, with an average of (28.88 ± 6.03) weeks. The age of the pregnant women ranged from 18 to 44 years, with an average age of 30.21 ± 4.07 years. The inclusion criteria were: ① singleton pregnancy; ② pregnant woman with definite last menstrual period, and consistent ultrasound gestational age and menstrual age; ③ absence of fetal malformations detected during prenatal ultrasound examinations; ④ No significant abnormalities observed in systemic or neurological examination by physicians in the Department of Child Healthcare on the 42nd day after birth. The exclusion criteria were: ① Pregnant women suffering from hypertension, diabetes, or other diseases affecting fetal growth and development; ② absence of signed consent forms from pregnant women; ③ twin or multiple pregnancies; ④ Fetal growth restriction or

structural malformations. This study was approved by the Medical Ethics Committee of our hospital. All pregnant women were aware of the content of this study and signed the informed consent form.

2.2. Instruments and methods

2.2.1. Instruments
This study was carried out using the color Doppler ultrasound diagnostic instrument (Voluson E8, GE, Austria), with the probe type C1-5-D and the probe frequency at 2–6 MHz.

2.2.2. Image acquisition methods and requirements
Routine prenatal ultrasound examinations were performed on the fetuses through the type of approach as transabdominal. The fetal spinal column was scanned continuously in the sagittal, coronal and transverse planes to exclude the abnormalities in the spinal cord and spinal column. In the lumbosacral region of the fetal spine, a midsagittal section was taken to simultaneously display the end of the conus medullaris, the ossification centers of each vertebral body in the lumbosacral region, and the skin of the fetal sacrococcygeal region.

2.2.3. Measurement methods
① New ranging method: The distance between the end of the fetal conus medullaris and the caudal end of the ossification center of the terminal vertebral body (Distance 1, D1), and the distance between the end of the conus medullaris and the intersection of the D1 extension and the caudal skin (Distance 2, D2) were measured. ② Horizontal ranging method: In the image displaying the midsagittal section of the fetal sacrococcygeal region, the measurement button was clicked and the Dist.2 Line was selected. After a vertical line, Line 1 was drawn through the end of the conus medullaris, and the OK button was clicked. Then, another vertical line, Line 2, was made through the caudal end of the ossification center of the terminal vertebral body by sliding the trackball, followed by the OK button clicking. The automatically measured data were the horizontal distance between the end of the conus medullaris and the caudal end of the ossification center of the terminal vertebral body, which was recorded as HD. All data were measured by senior sonographers three times, and averages were taken and recorded. A total of 50 fetuses were selected using simple random sampling, and image acquisition and data measurement were performed by different physicians for a repeatability test between two observers.

2.3. Statistical methods

The data were statistically analyzed using SPSS 25.0 and the measurement data were expressed as ($\bar{x} \pm s$). Linear regression was used to evaluate the correlations between D1, D2, HD and gestational age, and a linear regression equation was established, with R^2 representing their correlations. The ascending velocity of the conus medullaris was compared between adjacent gestational ages by the LSD test, and the repeatability between two observers was analyzed using the paired t-test. $P < 0.05$ was considered as statistically significant.

3. Results

The measure of HD is depicted in the sonographic image of a selected case, as presented in Fig. 1, the image displaying the midsagittal section of the fetal sacrococcygeal region. The distance from A to B is called Distance 1, D1 in short. Distance from A to C is called Distance 2, D2 in short. Distance

Fig. 1. Measurement of D1, D2 and HD ultrasound schematic diagram. The distance between A and B is D1. The distance between A and C is D2. The distance between a and b is HD. Point A (also marked as "a") stands for the end of the fetal conus medullaris, point B stands for the caudal end of the ossification center of the terminal vertebral body, point C as the intersection of the D1 extension and the caudal skin, point b as the intersection of the parallel line passing through point A (or a) and the vertical line passing through point B.
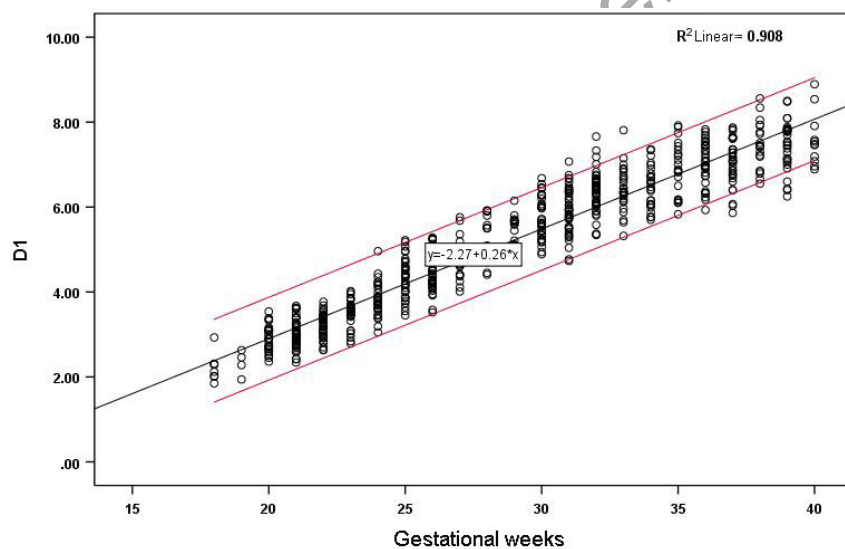

Fig. 2. Correlation between D1 and gestational age and reference range.

between a to b equals the horizontal distance from A level to B level, stands for HD. The determination of anatomical marks (A, B, C, a, b) in the images depends on the sonographer's experience.

The D1, D2 and HD of the 655 fetuses are shown in Figs 2–4. The measured values of fetal BPD, OFD, FL and HL are listed in the Supplementary Table. D1, D2 and HD were strongly correlated with gestational age and increased with gestational age. The correlation coefficients were $r = 0.953$ ($P < 0.001$), $r = 0.956$ ($P < 0.001$) and $r = 0.951$ ($P < 0.001$), respectively. The linear regression equations were D1 = $0.258 \times$ gestational age – 2.269 cm ($R^2 = 0.908$), D2 = $0.276 \times$ gestational age – 2.053 cm ($R^2 = 0.915$), and HD = $0.259 \times$ gestational age – 2.373 cm ($R^2 = 0.905$), respectively. The normal reference ranges of D1, D2 and HD are presented in Table 1. The median value of D1 increased from 2.23 cm at the gestational age of 18 weeks to 7.59 cm at the gestational age of 40 weeks. The median

Fig. 3. Correlation between D2 and gestational age and reference range.

Fig. 4. Correlation between HD and gestational age and reference range.

value of D2 increased from 2.69 cm at the gestational age of 18 weeks to 8.46 cm at the gestational age of 40 weeks. The median value of HD increased from 2.20 cm at the gestational age of 18 weeks to 7.54 cm at the gestational age of 40 weeks. The medians of D1, D2 and HD at different gestational weeks are displayed in Table 3.
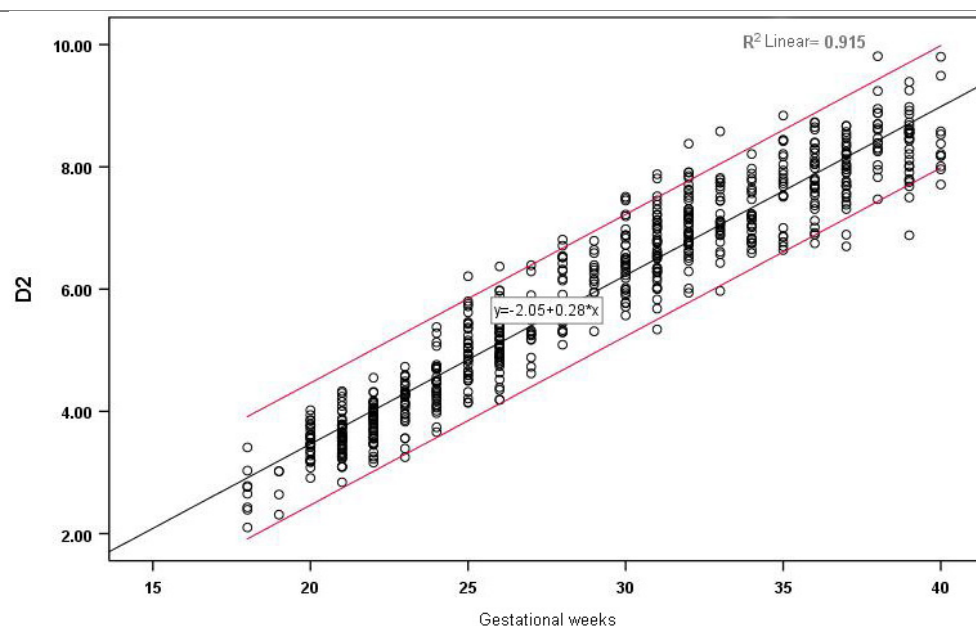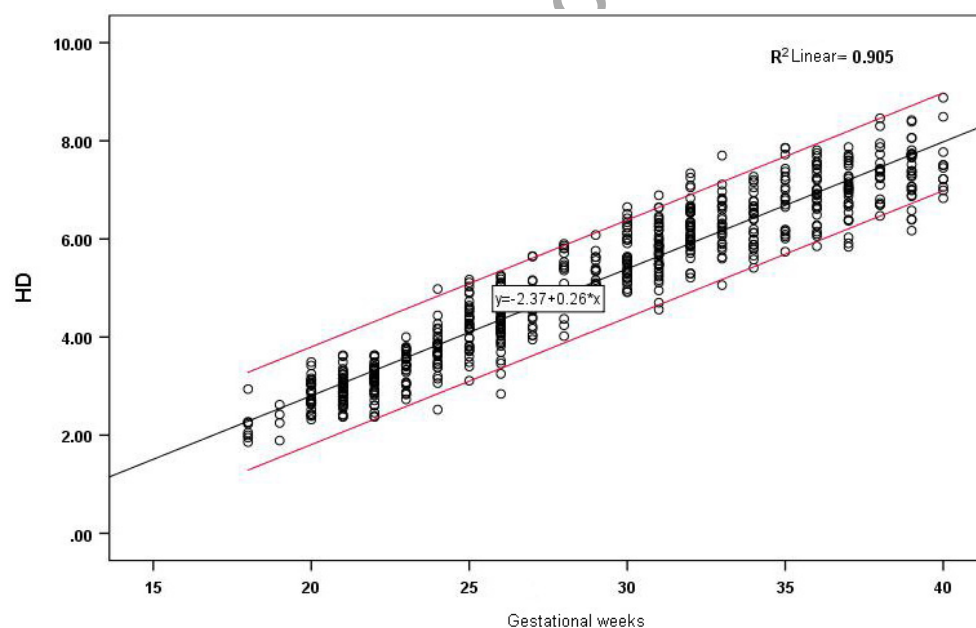
6   *X. Liu et al. / Ultrasound study of fetal conus medullaris position*

Table 1
Normal reference ranges of fetal D1, D2 and HD at gestational age of 18–40 weeks (cm)

Gestational age	D1							D2							HD						
	0.50%	2.50%	5%	50%	95%	97.50%	99.50%	0.50%	2.50%	5%	50%	95%	97.50%	99.50%	0.50%	2.50%	5%	50%	95%	97.50%	99.50%
18	1.38	1.59	1.69	2.23	2.77	2.87	3.08	1.65	1.90	2.03	2.69	3.36	3.49	3.74	1.32	1.53	1.64	2.20	2.75	2.86	3.07
19	1.57	1.75	1.84	2.33	2.81	2.91	3.09	1.86	2.08	2.19	2.75	3.31	3.42	3.63	1.50	1.69	1.79	2.30	2.80	2.90	3.09
20	2.15	2.33	2.42	2.91	3.40	3.49	3.68	2.78	2.96	3.04	3.50	3.95	4.04	4.21	2.04	2.23	2.33	2.84	3.36	3.45	3.65
21	2.16	2.36	2.47	3.00	3.54	3.64	3.85	2.73	2.94	3.05	3.59	4.14	4.24	4.45	2.18	2.36	2.46	2.95	3.44	3.53	3.71
22	2.48	2.66	2.75	3.21	3.67	3.75	3.93	3.03	3.22	3.32	3.82	4.32	4.42	4.61	2.31	2.50	2.60	3.12	3.63	3.73	3.93
23	2.66	2.86	2.96	3.50	4.04	4.14	4.35	3.21	3.43	3.55	4.14	4.73	4.84	5.07	2.55	2.75	2.86	3.40	3.94	4.05	4.25
24	2.83	3.07	3.19	3.82	4.44	4.57	4.80	3.41	3.67	3.80	4.46	5.13	5.26	5.51	2.58	2.86	3.00	3.73	4.46	4.60	4.88
25	3.14	3.42	3.57	4.33	5.08	5.23	5.51	3.70	4.02	4.18	5.00	5.82	5.98	6.29	2.95	3.25	3.41	4.23	5.05	5.21	5.52
26	3.42	3.69	3.83	4.53	5.24	5.38	5.64	3.97	4.26	4.41	5.19	5.96	6.11	6.41	3.04	3.36	3.52	4.36	5.19	5.35	5.67
27	3.51	3.81	3.97	4.76	5.55	5.70	6.00	4.24	4.52	4.67	5.42	6.17	6.32	6.60	3.37	3.67	3.83	4.64	5.46	5.61	5.92
28	3.91	4.23	4.40	5.25	6.11	6.27	6.60	4.56	4.91	5.08	5.98	6.88	7.06	7.40	3.64	4.00	4.18	5.11	6.05	6.23	6.58
29	4.48	4.71	4.83	5.43	6.04	6.15	6.38	5.05	5.30	5.43	6.09	6.76	6.89	7.14	4.37	4.59	4.71	5.30	5.89	6.00	6.22
30	4.46	4.76	4.92	5.73	6.53	6.69	6.99	5.12	5.45	5.62	6.49	7.36	7.53	7.86	4.39	4.69	4.85	5.65	6.45	6.61	6.91
31	4.52	4.85	5.02	5.90	6.77	6.94	7.28	5.26	5.60	5.78	6.69	7.60	7.77	8.12	4.46	4.78	4.94	5.79	6.64	6.80	7.12
32	5.08	5.38	5.53	6.33	7.13	7.29	7.59	5.76	6.08	6.24	7.08	7.92	8.08	8.40	4.98	5.28	5.43	6.23	7.03	7.19	7.49
33	5.10	5.42	5.58	6.42	7.26	7.42	7.74	5.81	6.14	6.31	7.18	8.06	8.23	8.56	4.92	5.26	5.43	6.33	7.22	7.40	7.74
34	5.19	5.50	5.66	6.46	7.27	7.42	7.73	6.07	6.35	6.49	7.22	7.96	8.10	8.38	5.01	5.34	5.51	6.37	7.23	7.40	7.72
35	5.28	5.67	5.87	6.89	7.90	8.10	8.49	6.02	6.42	6.62	7.67	8.72	8.92	9.32	5.19	5.58	5.79	6.83	7.87	8.07	8.46
36	5.70	6.02	6.18	7.01	7.85	8.01	8.33	6.38	6.73	6.91	7.82	8.74	8.92	9.27	5.55	5.88	6.06	6.94	7.83	8.00	8.34
37	5.70	6.03	6.20	7.06	7.93	8.10	8.42	6.69	6.99	7.14	7.93	8.72	8.87	9.17	5.62	5.95	6.12	6.98	7.85	8.01	8.34
38	5.99	6.34	6.52	7.45	8.38	8.56	8.91	7.15	7.47	7.64	8.51	9.38	9.55	9.88	5.95	6.28	6.46	7.35	8.25	8.42	8.76
39	5.95	6.31	6.50	7.45	8.40	8.59	8.95	6.94	7.28	7.45	8.35	9.25	9.42	9.76	5.90	6.26	6.44	7.38	8.32	8.50	8.86
40	5.95	6.35	6.55	7.59	8.63	8.84	9.23	6.80	7.20	7.41	8.46	9.51	9.71	10.11	5.91	6.30	6.50	7.54	8.58	8.78	9.17

Table 2
Repeatability test results of D1, D2 and HD between two physicians (cm, $\bar{x} \pm s$)

Measurer	Sample size	D1	D2	HD
Physician 1	50	4.95 ± 1.91	5.62 ± 2.05	4.89 ± 1.91
Physician 2	50	4.84 ± 1.95	5.52 ± 2.08	4.79 ± 1.94
t		1.738	1.799	1.691
P		0.089	0.078	0.097

Table 3
Fetal D1, D2 and HD at gestational age of 18–40 weeks ($\bar{x} \pm s$)

Gestational age	N	D1	P	D2	P	HD	P
18	8	2.23 ± 0.33	–	2.69 ± 0.41	–	2.20 ± 0.34	–
19	4	2.33 ± 0.30	0.73	2.75 ± 0.34	0.85	2.30 ± 0.31	0.73
20	29	2.91 ± 0.30	0.18	3.50 ± 0.28	0.00	2.84 ± 0.31	0.03
21	46	3.00 ± 0.33	0.41	3.59 ± 0.33	0.39	2.95 ± 0.30	0.36
22	44	3.21 ± 0.28	0.04	3.82 ± 0.31	0.02	3.12 ± 0.31	0.09
23	30	3.50 ± 0.33	0.01	4.14 ± 0.36	0.01	3.40 ± 0.33	0.01
24	32	3.82 ± 0.38	0.01	4.46 ± 0.41	0.01	3.73 ± 0.44	0.01
25	35	4.33 ± 0.46	0.00	5.00 ± 0.50	0.00	4.23 ± 0.50	0.00
26	51	4.53 ± 0.43	0.04	5.19 ± 0.47	0.07	4.36 ± 0.51	0.24
27	19	4.76 ± 0.48	0.07	5.42 ± 0.46	0.07	4.64 ± 0.50	0.03
28	21	5.25 ± 0.52	0.00	5.98 ± 0.55	0.00	5.11 ± 0.57	0.00
29	17	5.43 ± 0.37	0.24	6.09 ± 0.41	0.47	5.30 ± 0.36	0.24
30	33	5.73 ± 0.49	0.03	6.49 ± 0.53	0.01	5.65 ± 0.49	0.01
31	43	5.90 ± 0.53	0.11	6.69 ± 0.55	0.08	5.79 ± 0.52	0.20
32	44	6.33 ± 0.49	0.00	7.08 ± 0.51	0.00	6.23 ± 0.49	0.00
33	27	6.42 ± 0.51	0.44	7.18 ± 0.53	0.37	6.33 ± 0.55	0.41
34	27	6.46 ± 0.49	0.76	7.22 ± 0.45	0.76	6.37 ± 0.53	0.77
35	22	6.89 ± 0.62	0.00	7.67 ± 0.64	0.00	6.83 ± 0.63	0.00
36	31	7.01 ± 0.51	0.32	7.82 ± 0.56	0.25	6.94 ± 0.54	0.38
37	33	7.06 ± 0.53	0.68	7.93 ± 0.48	0.37	6.98 ± 0.53	0.74
38	19	7.45 ± 0.57	0.00	8.51 ± 0.53	0.00	7.35 ± 0.55	0.01
39	29	7.45 ± 0.58	0.98	8.35 ± 0.55	0.24	7.38 ± 0.57	0.86
40	11	7.59 ± 0.64	0.39	8.46 ± 0.64	0.52	7.54 ± 0.63	0.35

Notes: P, comparison of D1, D2 and HD with means at the previous gestational week.

The repeatability test results of D1, D2 and HD between two physicians are displayed in Table 2, demonstrating no statistically significant differences in the observations. The measurement repeatability of the distances between different operators was high, indicating that this method is not affected by physiological curvature of the spine and exhibits simplicity and high repeatability. Among the ratios of D1, D2 and HD to commonly used growth parameters, D2/FL tended to stabilize after 20 weeks of gestation, with values consistently greater than 1 (Table 4).

Through analysis of the measured values, a linearly positive correlation was found between HD and gestational age, with the linear regression equation of HD $= 0.259 \times$ gestational age $- 2.373$ cm ($R^2 = 0.905$). The analysis of HD measured at 18–40 + 6 weeks showed statistically significant differences between two adjacent gestational ages at 19–20 + 6 weeks, 21–22 + 6 weeks, 22–23 + 6 weeks, 23–24 + 6 weeks, 24–25 + 6 weeks, 26–27 + 6 weeks and 27–28 + 6 weeks ($P < 0.05$). During this period, the conus medullaris ascended rapidly. There were also statistically significant differences between adjacent gestational ages at 29–30 + 6 weeks, 31–32 + 6 weeks, 34–35 + 6 weeks and 37–38 + 6 weeks ($P < 0.05$). No statistically significant differences were observed between other adjacent gestational ages ($P > 0.05$) (as seen in Table 3), suggesting that the conus medullaris ascends rapidly at 19–28 weeks, and then gradually and intermittently after 28 weeks. According to the analysis of the ratios of HD to various

Table 4
Fetal D1/FL, D2/FL and HD/FL at the gestational age of 18–40 weeks ($\bar{x} \pm s$)

Gestational age	N	D1/FL	P	D2/FL	P	HD/FL	P
18	8	0.81 ± 0.12	–	0.98 ± 0.17	–	0.79 ± 0.12	–
19	4	0.78 ± 0.10	0.55	0.92 ± 0.11	0.24	0.77 ± 0.10	0.60
20	29	0.87 ± 0.08	0.37	1.04 ± 0.07	0.01	0.85 ± 0.09	0.07
21	46	0.86 ± 0.09	0.47	1.02 ± 0.10	0.31	0.84 ± 0.09	0.64
22	44	0.85 ± 0.08	0.70	1.01 ± 0.08	0.52	0.83 ± 0.09	0.43
23	30	0.86 ± 0.07	0.67	1.01 ± 0.07	0.96	0.83 ± 0.07	0.74
24	32	0.89 ± 0.09	0.11	1.04 ± 0.09	0.20	0.87 ± 0.10	0.08
25	35	0.94 ± 0.09	0.10	1.09 ± 0.10	0.03	0.92 ± 0.10	0.14
26	51	0.95 ± 0.08	0.87	1.08 ± 0.09	0.71	0.91 ± 0.10	0.48
27	19	0.95 ± 0.10	0.96	1.08 ± 0.09	0.99	0.92 ± 0.10	0.53
28	21	1.00 ± 0.10	0.34	1.14 ± 0.10	0.22	0.98 ± 0.11	0.59
29	17	0.99 ± 0.06	0.52	1.11 ± 0.07	0.20	0.96 ± 0.06	0.60
30	33	1.01 ± 0.09	0.41	1.14 ± 0.10	0.18	0.99 ± 0.09	0.22
31	43	1.00 ± 0.09	0.79	1.14 ± 0.09	0.79	0.98 ± 0.08	0.62
32	44	1.04 ± 0.08	0.20	1.17 ± 0.09	0.11	1.03 ± 0.08	0.23
33	27	1.02 ± 0.08	0.23	1.14 ± 0.08	0.14	1.00 ± 0.08	0.29
34	27	1.00 ± 0.08	0.30	1.11 ± 0.06	0.15	0.98 ± 0.08	0.33
35	22	1.04 ± 0.08	0.55	1.16 ± 0.08	0.55	1.03 ± 0.09	0.04
36	31	1.04 ± 0.07	0.78	1.15 ± 0.08	0.87	1.02 ± 0.08	0.74
37	33	1.02 ± 0.08	0.42	1.15 ± 0.09	0.79	1.01 ± 0.08	0.42
38	19	1.05 ± 0.09	0.19	1.19 ± 0.08	0.06	1.04 ± 0.08	0.24
39	29	1.04 ± 0.07	0.73	1.16 ± 0.07	0.23	1.03 ± 0.07	0.78
40	11	1.04 ± 0.08	0.99	1.14 ± 0.10	0.42	1.03 ± 0.08	0.95
Total	655	0.96 ± 0.11		1.10 ± 0.10		0.94 ± 0.12	

Notes: P, comparison of D1/FL, D2/FL and HD/FL with means at the previous gestational week.

biological measures, although the ratios increased with gestational age, most of the differences between adjacent gestational ages were not statistically significant. Notably, HD/FL remained relatively stable, and consistently exceeded 0.8 after 20 weeks (Table 4).

4. Discussion

The entire research took two years to complete, including one year of data collection and one year of data organization, analysis, and follow-up study.

Though identified as a main cause of TCS, the prenatal diagnosis of closed skin lesions caused by fetal diseases still poses challenges. However, as a common characteristic, the close skin lesion-leading diseases commonly result in the low position of the conus medullaris. Thus it is diagnostically valuable to evaluate the position of the conus medullaris in prenatal ultrasound examination [9]. In the research by Luo et al. [10], the conus medullaris positions in 974 normal fetuses ranging from 15 to 41 weeks of gestation and 46 fetuses with TCS were enrolled and analyzed with a new ranging method. They stated that D1 and D2 exhibited a linear correlation with gestational age, with fitting equations of D1 $= 0.251\text{GA} - 2.265$ cm ($R^2 = 0.926$, $P < 0.001$) and D2 $= 0.267\text{GA} - 1.812$ cm ($R^2 = 0.928$, $P < 0.001$), for both D1 and D2, there were statistically significant differences between the measurements of normal and abnormal groups. Therefore, prenatal measurements of D1 and D2 contribute to the diagnosis of TCS. Zhai et al. [11] observed a linearly positive correlation between the distance from the conus medullaris to the first sacral vertebra (CM-S1) and gestational age, the linear regression equation of CM-S1 $= 1.57 \times$ gestational age $- 16.43$ ($R^2 = 0.89$). In the TCS group, the fetal CM-S1 was smaller

than the 5th percentile of the corresponding gestational age. Shen et al. [12] obtained the linear regression equation using the trajectory ranging method, where the CD value of the trajectory method was defined as the distance between the end of the conus medullaris and the distal ossification center of the spine. The equation derived was CD value of the trajectory method $= 0.037GA - 2.275$ ($R^2 = 0.885$, $P < 0.001$).

In the present study, we measured the distance between the end of the fetal conus medullaris and the caudal end of the ossification center of the terminal vertebral body (referred to as Distance 1, D1), as well as the distance between the end of the conus medullaris and the intersection of the D1 extension and the caudal skin (referred to as Distance 2, D2). Analysis of the measured values revealed a rapid ascent of the conus medullaris between 19–28 weeks, followed by a gradual and intermittent ascent after 28 weeks (as shown in Table 3), which corroborated the findings obtained through the horizontal ranging method. The linear regression equations derived from our study were D1 $= 0.258 \times$ gestational age $- 2.269$ cm ($R^2 = 0.908$) and D2 $= 0.276 \times$ gestational age $- 2.053$ cm ($R^2 = 0.915$), which are approximate to the equations obtained by Luo et al. Additionally, Luo et al. recommend the use of FL/D2 with a cutoff of 1 as the diagnostic criterion, which exhibited a sensitivity of 97.9% and specificity of 87%. Our study analyzed the ratios of D1 and D2 to various growth parameters and revealed that D2/FL remained relatively stable and higher than 1 after 20 weeks of gestation, aligning with the study of Luo et al. Based on these results, we conducted an evaluation of the vertebral level corresponding to the end of the conus medullaris in 93 fetuses (14.5%) with D2/FL < 1, employing the caudal vertebral counting method. During the early stage of mid-pregnancy, the conus medullaris was primarily situated between the lower edge of L4 and the middle segment of L3 among the 93 fetuses. Subsequently, all 93 fetuses underwent close follow-up to monitor the ascent of their conus medullaris, which reached a level above L3 between 28 and 39 weeks of gestation. Among these cases, four fetuses displayed a gradual ascent, ultimately reaching the lower edge, middle segment, or upper edge of L3 at 34, 37, 37, and 39 weeks of gestation, respectively. Importantly, no abnormal performance or complications were observed during the follow-up period ranging from 5 to 35 months.

Notably, previous research has demonstrated that ultrasound exhibits similar sensitivity to magnetic resonance imaging (MRI) in detecting spinal abnormalities [13,14]. Consequently, ultrasound presents promising prospects for evaluating the position of the fetal conus medullaris. The proposed horizontal ranging method introduced in our study offers convenience, quick operation, and facilitates the efficient prenatal evaluation of the low position of the conus medullaris, effectively excluding the possibility of TCS in fetuses.

However, it is essential to acknowledge that this is a single-center prospective study with certain limitations. The sample size is small, and the subjects constituted only a specific population within the region. Future clinical endeavors should focus on expanding the observed populations across multiple regions and enhancing follow-up monitoring to further strengthen the validity and applicability of our findings. Additionally, the novel methodology of we raised in the study can also combine with artificial intelligence (AI) in clinical practice.

To locate the conus medullaris through ultrasound remains a challenge, the failure always results from the difficulty to capture image due to fetal movement [15], which leads to time waste and unnecessary energy consumption of the physicians. AI presents superior advantages in the process of its rapid development [16,17], in the field of obstetry, the applications of AI in the recognition of medical images detected by ultrasound and the measurements of obstetric parameters have become increasingly apparent [18].

Currently, AI contributes to the automatic recognition of multi-organ diverse sectional views, including the head, face, abdomen, and heart of the fetus [19–22]. The detection by AI accurately measures fetal

biometric parameters, inclusive of biparietal diameter, head circumference, abdominal circumference, and femur length, to observe fetal abnormalities [23]. With the development of deep learning methods and continuous improvement of intelligent models, AI has achieved intelligent segmentation of images and measurement of fetal biometric parameters during the continuous scanning process [24–26]. As a result, there is great potential on the AI-driven automatic segmentation and measurement of the fetal conus medullaris, enabling fast and efficient identification of its position and any potential abnormalities during the scanning process.

5. Conclusion

This study introduces the innovative horizontal ranging method for evaluating the fetal conus medullaris position. By using ultrasound images with clear anatomical landmarks, the HD measurement provides a more straightforward and reliable assessment, less affected by physiological curvature of the spine. The significance of this research lies in its potential to detect conus medullaris abnormalities early on, like TCS, enabling timely postpartum diagnosis and intervention to prevent irreversible neurological damage in infants. The simplicity and ease of implementation make the horizontal ranging method suitable for routine prenatal ultrasound examinations.

We also made a start on the establishment of normal reference values, so medical professionals can confidently interpret results and identify potential issues, paving the way for the method's broader adoption. As AI and medical imaging advance, further exploration and application of the HD measuring method offer promising prospects for enhanced prenatal care, ensuring better outcomes for infants at risk of related conditions. Overall, this study contributes valuable insights to prenatal diagnostics, enhancing the understanding and management of fetal conus medullaris anomalies.

Ethics statement

This study was conducted in accordance with the Declaration of Helsinki and approved by the ethics committee of Hebei Medical University Third Hospital. Written informed consent was obtained from the participants or legal guardians.

Availability of data and materials

All data generated or analyzed during this study are included in this article. Further enquiries can be directed to the corresponding author.

Competing interests

None of the authors has any personal, financial, commercial, or academic conflicts of interest to report.

Funding

Author contributions

LXP and LP conceived the study and YYM and TC participated in its design and data analysis and statistics. All authors helped draft the manuscript and read and approved the final version.

Acknowledgments

None to report.

Supplementary data

The supplementary files are available to download from http://dx.doi.org/10.3233/THC-230332.

References

[1] Rodríguez MA, Prats P, Rodríguez I, Comas C. Prenatal evaluation of the fetal conus medullaris on a routine scan. Fetal Diagn Ther. 2016; 39(2): 113-6. doi: 10.1159/000441295.

[2] Dale K, Martí E. Introduction to the special section: Spinal Cord a model to understand CNS development and regeneration. Dev Biol. 2017 Dec 1; 432(1): 1-2. doi: 10.1016/j.ydbio.2017.10.005.

[3] Hertzler DA 2nd, DePowell JJ, Stevenson CB, Mangano FT. Tethered cord syndrome: A review of the literature from embryology to adult presentation. Neurosurg Focus. 2010 Jul; 29(1): E1. doi: 10.3171/2010.3.FOCUS1079.

[4] Jing B, Zhang H, Sun Y. Prenatal assessment and pregnancy outcomes of foetal low-lying conus medullaris using 3D ultrasound. BMC Pregnancy Childbirth. 2022 Dec 23; 22(1): 961. doi: 10.1186/s12884-022-05244-3.

[5] Paladini D, Malinger G, Birnbaum R, Monteagudo A, Pilu G, Salomon LJ, Timor-Tritsch IE. ISUOG Practice Guidelines (updated): Sonographic examination of the fetal central nervous system. Part 2: Performance of targeted neurosonography. Ultrasound Obstet Gynecol. 2021 Apr; 57(4): 661-671. doi: 10.1002/uog.23616.

[6] Qian BL, Xie LM. Progress in ultrasound localization method of conus medullaris end position. Biomedical Engineering and Clinical Medicine. 2017; 21(05): 559-563. doi: 10.13339/j.cnki.sglc.20170906.024.

[7] Yirizhati AL, Wang ZL. Research progress in occult tethered cord syndrome. Chinese Journal of Clinical Neurosurgery. 2021; 26(12): 967-969. doi: 10.13798/j.issn.1009-153X.2021.12.024.

[8] Hoopmann M, Abele H, Yazdi B, Schuhmann MU, Kagan KO. Prenatal evaluation of the position of the fetal conus medullaris. Ultrasound Obstet Gynecol. 2011 Nov; 38(5): 548-552. doi: 10.1002/uog.8955.

[9] Ramirez Zegarra R, Volpe N, Bertelli E, Amorelli GM, Ferraro L, Schera GBL, Cromi A, di Pasquo E, Dall'Asta A, Ghezzi F, Frusca T, Ghi T. Three-dimensional sonographic evaluation of the position of the fetal conus medullaris at first trimester. Fetal Diagn Ther. 2021; 48(6): 464-471. doi: 10.1159/000516516.

[10] Luo DD, Huang Y, Li SL, Tian XX, Wen HX, Yuan Y, Yang SH, Bi JR, Xiao ZL, Chen CY, Yu R. The new approach in the location of the fetal conus medullaris and its application in tethered cord syndrome. Chinese Journal of Ultrasonography. 2018; 27(3): 252-258. doi: 10.3760/cma.j.issn.1004-4477.2018.03.016.

[11] Zhai J, Cai AL, Sun HB, Jin CL, Zhao D. A new method for sonographic quantitative evaluation of fetal conus medullaris in routine 2D scans. Chinese Journal of Ultrasound in Medicine. 2018; 34(9): 818-820. doi: 10.3969/j.issn.1002-0101.2018.09.019.

[12] Shen M, Wang LX, Li JN, Xu H, Li QY. Diagnostic value of trace method of ultrasound examination for locating conus medullaris in fetal tethered spinal cord. Academic Journal of Chinese Pla Medical School. 2022; 43(6): 628-633, 653. doi: 10.3969/j.issn.2095-5227.2022.06.003.

[13] He SZ, Lv GR, Liu SL, Ruan JX. Prenatal ultrasound evaluation of the position of conus medullaris for the diagnosis of tethered cord syndrome. Ultrasound Q. 2016 Dec; 32(4): 356-360. doi: 10.1097/RUQ.0000000000000230.

[14] Zhao D, Wei Q, Cai A, Xie L, Wang B, Wang X. Prenatal assessment of the position of fetal conus medullaris as a predictor of fetal spinal lesions. J Ultrasound Med. 2018 Jan; 37(1): 201-207. doi: 10.1002/jum.14326.

[15] Li C, Ma Y. A meta-analysis of pregnancy outcomes in the diagnosis of isolated foetal renal parenchyma by prenatal ultrasonography. Technol Health Care. 2023; 31(4): 1393-1405. doi: 10.3233/THC-220690. PMID: 36872810.

[16] Hafizović L, Čaušević A, Deumić A, Becirovic LS, Pokvic LG, Badnjevi A. The Use of Artificial Intelligence in Diagnostic Medical Imaging: Systematic Literature Review. 2021 IEEE 21st International Conference on Bioinformatics and Bioengineering (BIBE), Kragujevac, Serbia. 2021; pp. 1-6. doi: 10.1109/BIBE52308.2021.9635307.

[17] Mujkić A, Baralić E, Ombašić A, Bećirović LS, Pokvić LG, Badnjević A. Machine Intelligence in Biomedical Data Modeling, Processing, and Analysis. 2022 11th Mediterranean Conference on Embedded Computing (MECO), Budva, Montenegro. 2022; pp. 1-10. doi: 10.1109/MECO55406.2022.9797164.

[18] Lewandowski N, Koller B. Transforming medical sciences with high-performance computing, high-performance data analytics and AI. Technol Health Care. 2023; 31(4): 1505-1507. doi: 10.3233/THC-237000.

[19] Yang X, Wang X, Wang Y, Dou H, Li S, Wen H, Lin Y, Heng PA, Ni D. Hybrid attention for automatic segmentation of whole fetal head in prenatal ultrasound volumes. Comput Methods Programs Biomed. 2020 Oct; 194: 105519. doi: 10.1016/j.cmpb.2020.105519.

[20] Liu Z, Wang X, Lv G, Du Y, Liu P, Wu X, He Z. Study on artificial intelligence automatic identification of standard fetal facial ultrasound sections. Chinese Journal of Medical Physics. 2021; 38(12): 1575-1578. doi: 10.3969/j.issn.1005-202X.2021.12.021.

[21] Kim B, Kim KC, Park Y, Kwon JY, Jang J, Seo JK. Machine-learning-based automatic identification of fetal abdominal circumference from ultrasound images. Physiol Meas. 2018 Oct 22; 39(10): 105007. doi: 10.1088/1361-6579/aae255.

[22] Luo G, Pan S, Qiao S, Pang S, Chen T, Sun L, Dong Y. Deep learning technology for automatic recognition of fetal echocardiography images. The Journal of Practical Medicine. 2022; (14): 1830-1833. doi: 10.3969/j.issn.1006-5725.2022.14.022.

[23] Ding H, Zheng M, Chen L, Wang B. Measurement of fetal growth and development indicators in ultrasound images based on image processing. Chinese Journal of Biomedical Engineering. 2018; 24(5): 342-346. doi: 10.3760/cma.j.issn.1674-1927.2018.05.008.

[24] Guo W, Luo D, Xu H, Liu Y, He H, Tan H, Li S. Novel intelligent ultrasound smart fetus advanced (SFA) technique for automatic distinguishing and acquiring fetal standard sections. Chinese Journal of Medical Imaging Technology. 2023; 39(01): 65-69. doi: 10.13929/j.issn.1003-3289.2023.01.014.

[25] Ghelich Oghli M, Shabanzadeh A, Moradi S, Sirjani N, Gerami R, Ghaderi P, Sanei Taheri M, Shiri I, Arabi H, Zaidi H. Automatic fetal biometry prediction using a novel deep convolutional network architecture. Phys Med. 2021 Aug; 88: 127-137. doi: 10.1016/j.ejmp.2021.06.020.

[26] Zhou S, Jin Q, Jiang X, Wang R, Wang B, Li J, Yao H, Yang Y, Gao W, Zhang W, Cao W. Application of remote fetal heart rate monitoring via internet in late pregnancy during the COVID-19 pandemic. Technol Health Care. 2023; 31(4): 1105-1117. doi: 10.3233/THC-220700.